Superhydrophobic Transparent Surface of Nanostructured Poly(Methyl Methacrylate) Enhanced by a Hydrolysis Reaction

E. K. Her,† T.-J. Ko,† B. Shin, H. Roh, W. Dai, W. K. Seong, H.-Y. Kim, K.-R. Lee, K. H. Oh, M.-W. Moon*

We report a method to create a self-cleaning, transparent surface on poly(methyl methacrylate) (PMMA) using a dry etching with CF_4 plasma and a subsequent hydrolysis process with water immersion. During the CF_4 plasma treatment, nanoscale pillar structures were formed and its aspect ratio tended to increase. However, the transparency was reduced due to the deposition and the accumulation of undesired capping layers, which cover the structures. The hydrolysis was used to remove the capping layers of metal fluoride. As a result, the surface improves their clarity based on the transmittance up to 95%, because the reflectivity was reduced. With a subsequent hydrophobic coating, a superhydrophobic surface was achieved showing robust anti-wetting and anti-dewing effects.

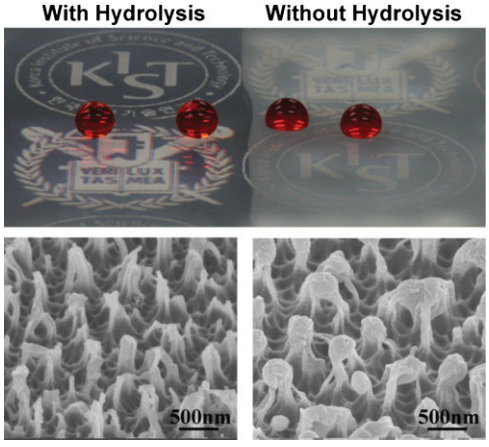

1. Introduction

Demand is increasing for functional surfaces with both superhydrophobicity and transparency in a range of optical fields. Examples include optics, windows for many recent electronic devices, and solar cell panels, all of which require high transmittance or transparency. However, a major difficulty when developing transparent superhydrophobic surfaces arises from the light scattering that is naturally induced by the surface roughness, which is detrimental to sustaining superhydrophobicity as well as avoiding wetting or dewing in the event of water condensation. Recently, highly transparent, thermoplastic polymers are gaining interest as glass is gradually being replaced. These polymers have several advantages over glass, such as significant weight reduction, greater impact strength, better molding options, and cost-savings in mass production. Among these polymers, poly(methyl methacrylate) (PMMA), a transparent polymer, is one of the most convenient and frequently used polymers in optic or medical devices, such as contact lenses, bone cement, and dental impression materials due to its high clarity.[1] Several novel methods to increase the transparency or to decrease the reflectivity of super-

Dr. E. K. Her, T.-J. Ko, B. Shin, Dr. W. Dai, Dr. W. K. Seong, Dr. K.-R. Lee, Dr. M.-W. Moon
Institute of Multidisciplinary Convergence of Materials, Korea Institute of Science and Technology, Seoul 136-791, Republic of Korea
E-mail: mwmoon@kist.re.kr
Dr. E. K. Her, T.-J. Ko, H. Roh, Prof. K. H. Oh
Department of Materials Science and Engineering, Seoul National University, Seoul 151-742, Republic of Korea
B. Shin, Prof. H.-Y. Kim
School of Mechanical and Aerospace Engineering, Seoul National University, Seoul 151-742, Republic of Korea
†These two authors have contributed equally to this work.

DOI: 10.1002/ppap.201200131

hydrophobic surfaces on PMMA have been developed by utilizing relevant hydrophobic coatings or structuring techniques.[2,3] Plasma-based surface treatments have been especially well-adapted for creating nanoscale roughness on various polymers such as polystyrene or PMMA.[2–5] Along with several precursors for a plasma treatment on polymeric materials, such as oxygen or Ar, fluorine-containing gas species such as CF_4 or C_4F_8 have been used for nanopatterns by selective etching when forming a local residue as an etching mask in a mechanism similar to that used to form high-aspect-ratio nanopatterns on Si (known as black silicon).[6–8] Fluorine-containing gases such as CF_4 are widely used at low gas pressures during plasma deposition and the etching of silicon and for insulating substrates such as PMMA.[8–11] However, the residues induced by fluorination may reduce the transparency as well as the hydrophobicity due to the formation of undesirable capping layers on top of the nanopatterns, as reported in several articles.[9–11] Mundo et al.[12] reported that CF_4 plasma-etched polycarbonate and polystyrene have higher optical reflectance levels compared to O_2 plasma-etched samples due to the relatively blunt nanostructures that are formed.

In this work, we provide a novel method to fabricate transparent, superhydrophobic PMMA with nanoscale pillars having a width of <200 nm and a height of approximately 500 nm using a CF_4 plasma treatment and a subsequent hydrolysis process via water immersion. The pillar morphology on the surface of the PMMA formed by the CF_4 plasma treatment was developed at certain accelerating voltages and treatment durations. A hydrophobic coating with a low surface energy of hexamethyldisiloxane (HMDSO) was then formed on the nanopillar surfaces to improve the self-cleaning ability. It was also observed that with an increase of the aspect ratio, defined as the ratio of the height over the diameter of the pillar, the pillar structures became clustered, after which the transparency was degraded due to the light scattering by these clusters, as shown in Figure 1. This is similar to the CF_4 plasma-induced nanostructures reported on polystyrene and Si.[9–11] These capping layers were successfully removed through hydrolysis during a water immersion process, resulting in the nanostructures having a diameter shorter than the optical wavelength of visible light, which improved the clarity.

A surface analysis of the plasma-treated surfaces was conducted to examine the surface characteristics that were altered with and without the hydrolysis process. The samples treated with the CF_4 plasma treatment were immersed in water, which removed the fluorine-rich clusters that had formed on the top of the nanopillars through a hydrolysis reaction. Water contact angle (CA) and contact angle hysteresis (CAH) measurements, as well as water condensation experiments, were performed to characterize the effect on the hydrophobicity on the wettability and the nucleation/growth of the water droplets, respectively. The change in the optical transmittance based on the UV–Vis spectra of PMMA samples with various plasma durations was also investigated to examine the hydrolysis effect.

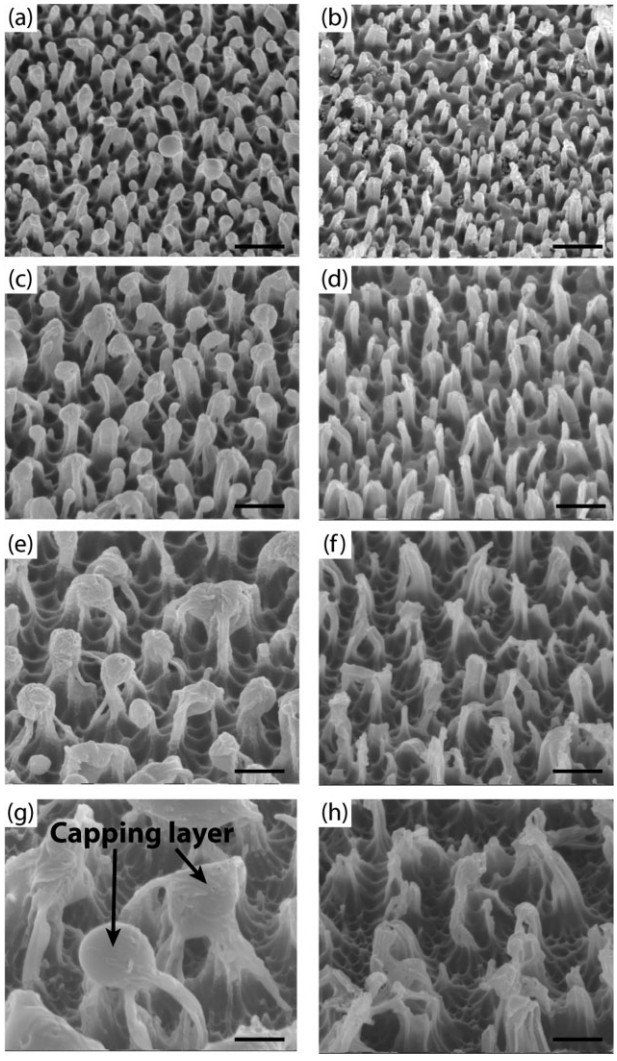

Figure 1. SEM images of surface morphologies with different plasma durations without water immersion (left) and with water immersion (right) on PMMA. The plasma duration varied as follows: (a) and (b) for 10 min, (c) and (d) for 20 min, (e) and (f) for 30 min, and (g) and (h) for 60 min. Scale bars are 500 nm.

2. Experimental Section

2.1. Sample Preparation

Commercially available PMMA, which is used for a light guide plate in TFT-LCDs (HP202, LG MMA, Rep. Korea) with a tensile strength of 720 $kg \cdot cm^{-2}$ (ASTM D638) and a density of 1.18 $g \cdot cm^{-3}$ (ASTM

DOI: 10.1002/ppap.201200131

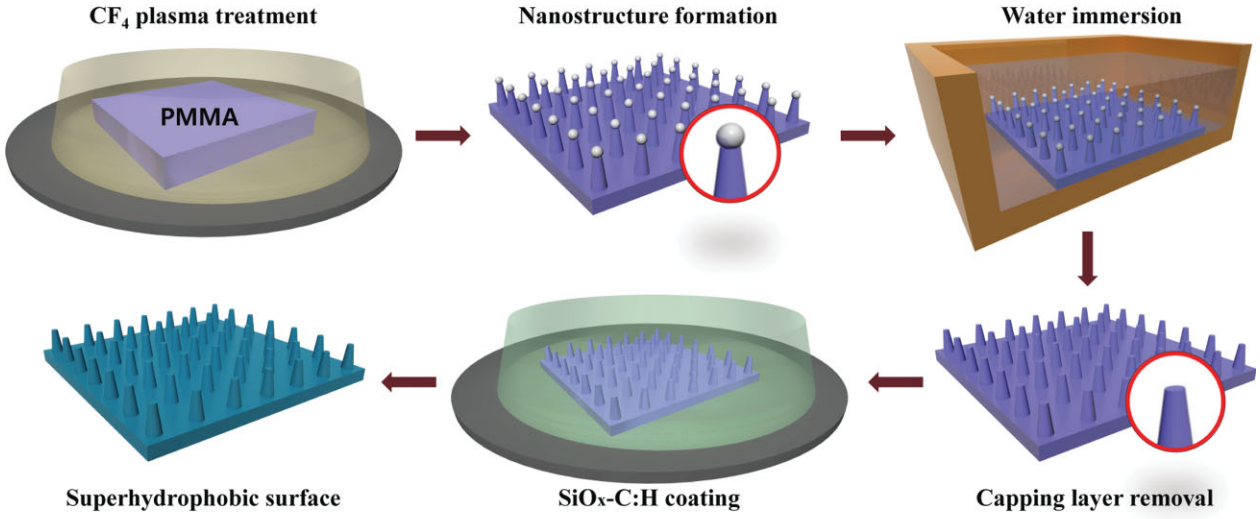

Figure 2. A schematic illustration of the fabrication procedure for superhydrophobic, transparent PMMA surfaces. Water immersion was employed to remove the capping layer (colored in white); thus, the diameter of the nanostructure was reduced.

D792) at room temperature, was cut into sections $30 \times 30 \times 4\,mm^3$ in size. Prior to the surface modification, all PMMA sections were cleaned thoroughly with methanol and triply deionized (DI) water to remove any surface contamination, after which they were dried with a N_2 gas blower. To fabricate superhydrophobic PMMA surfaces, plasma etching followed by a water immersion treatment (or hydrolysis process) and a coating process were conducted, as shown in Figure 2. The PMMA samples were etched using a glow discharge of CF_4 gas with the treatment duration ranging from 5 to 60 min using radio-frequency plasma-enhanced chemical vapor deposition (RF-PECVD). The gas pressure and the bias voltage were maintained at 20 mTorr and $-600\,V_b$, respectively. The samples were then immersed in DI water for the hydrolysis reaction for 10 min. To check the hydrolysis process in the water bath, the pH values of the water were measured before and after the immersion of the treated samples. To lower the surface energy of the nanostructured surfaces, a hydrophobic material (SiO_x–C:H film) was deposited onto the surface using a precursor of HMDSO in PECVD.[13–15] The gas pressure was fixed at 10 mTorr, the bias voltage was set to $-400\,V_b$, and the coating time was 5 s, which is equivalent to a thickness of 5 nm on a flat surface.

2.2. CA and CAH Measurements

We characterized the wettability of the nanostructured PMMA surfaces by measuring the CA and CAH of the DI water droplets. For these measurements, droplets with a volume of approximately 5 μL (with radii of approximately 1 mm) were gently deposited on the substrates using a microsyringe. The advancing CA was measured by adding a DI water sessile drop (~5 μL) and the receding CA was measured by the removal of the water from a DI water sessile drop. The CAH was calculated as the difference between the measured advancing and receding CAs. All measurements were taken using a contact angle goniometer (Rame-Hart, NJ, USA) in ambient air at 15 °C with a relative humidity of 20–35%. The reported CA values were determined by averaging the measurements from five different spots on each sample. Also, the falling motion of the water droplets on the plasma-treated and hydrophobic coated PMMA was observed with a high-speed video camera (Photron APX-RS, Photron, Marlow, UK) recording images at a rate of 500 frames per second.

2.3. SEM, XPS, and ESEM Analysis

The nanostructures on the PMMA surfaces were observed with a scanning electron microscope (SEM, Nova NanoSEM 200, FEI, OR, USA). Compositional analysis was performed with X-ray photoelectron spectroscopy (XPS, PHI 5800, ESCA System) to investigate the chemical change from the hydrolysis reaction on the plasma-treated PMMA. An Al Kα (1 486.6 eV) X-ray source was used as the excitation source, and the anode was maintained at 250 W, 10 kV, and 27 mA at a chamber pressure of 2.67×10^{-8} Pa with a beam spot size of 400 μm × 400 μm. The peak position was calibrated using the C1s peak at 284.6 eV. The UV–Vis measurements were taken in a wavelength range of 300–800 nm using a spectrophotometer (Lambda 20, Perkin-Elmer, MA, USA) at room temperature. The spectra were recorded with air as a reference.

Heterogeneous nucleation and the subsequent condensation process of the water droplets on the solid surfaces were observed with an environmental scanning electron microscope (ESEM, XL-30 FEG, FEI, OR, USA). Superhydrophobic PMMA (etched by CF_4 plasma for 30 min followed by water immersion for 10 min and coated with SiO_x–C:H for 5 s) and hydrophobic PMMA (etched by CF_4 plasma for 30 min and coated with SiO_x–C:H for 5 s) were used to examine the hydrolysis effect. The substrate temperature was maintained at 275 K by a cold stage module. The initial chamber pressure was 5.2 Torr, which is below the saturation pressure of water of 275 K; it was increased gradually to 5.6 Torr to induce water nucleation on the surfaces. Micrographs of the condensation behavior were taken every 10 s during the ESEM observation process.

3. Results and Discussion

3.1. Characterization of the Surface Morphology

Several droplets of water are placed on the surfaces before and after the hydrolysis process, as shown in the optical image in Figure 3. The left side of the PMMA surface underwent the hydrolysis process, showing a higher wetting angle and better transparency such that images in black and white underneath can be seen. The right side, having not undergone the hydrolysis process, shows a lower CA and a more blurred background image. Figure 1 shows SEM micrographs of the surface morphology of the CF_4 plasma-treated PMMA samples with and without the hydrolysis process. As the CF_4 plasma duration increased from 5 to 60 min, the aspect ratio of the PMMA pillars increased (see the left column in Figure 1) while the PMMA pillars became clustered and were capped by a number of mushroom-shaped layers. This was also observed in previous reports with polystyrene and Si.[9–11] Kim et al.[8] reported that CF_4 plasma-treated Si surfaces have clusters with local residue films from the CF_4 plasma, which form the nanoscale pillar structure.

It was observed that with the water immersion process, the capping layers are clearly removed and only the PMMA pillar structure remains. The PMMA pillar structure is more upright, as shown in the right column in Figure 1, the mechanism of which is discussed below. For a CF_4 plasma duration lower than 30 min, the diameter of pillar patterns increases to 200 nm; for a duration of 60 min, the pillar diameter increases to more than 400 nm due to agglomeration, and several bunches of pillars are formed. It was noted that when PMMA surfaces were treated with CF_4 plasma with more than 30 min, the pillars were bent and became aggregated due to the limitation of the Young's modulus and the Van der Waals force.[16]

It was reported that PMMA, as a relatively hard polymer, forms several different nanoscale morphologies under a variety of ion beam or plasma conditions, such as holes, cones, pillars, hairs, or bubbles, due to bond scission or cross-linking.[17–19] The formation of free radicals, recombination and the scission of bonds, cross-linking and various oxidation reactions take place during the ion beam irradiation process on PMMA. The observed evolution of the surface nanostructure during the CF_4 plasma etching is presumably due to the local deposition of an inhibitor that suppresses the etching.[14] High-energy electrons collide with gas molecules and create new species during plasma treatment; therefore, many physical and chemical reactions occur, such as ionization, electronic excitation, and molecular fragmentation.

3.2. Surface Analysis Using XPS

An XPS analysis was carried out to determine the chemical changes on the CF_4 plasma-treated PMMA surfaces treated for 30 min with and without water immersion, as shown in Figure 4 and Table 1. Figure 4a shows the XPS wide energy spectra of a pristine PMMA sample and of plasma-treated PMMA samples. The wide energy spectrum of the pristine PMMA shows peaks at the expected positions that correspond to common PMMA.[20] The plasma-treated PMMA surface shows not only a fluorine-related peak but also minor peaks of Fe and Cr due to the sputtering from the chamber wall as well as the cathode plate, which were made of the stainless steel. The overall fluorine content of the CF_4 plasma-treated PMMA treated for 30 min was measured and found to decrease from 51.8% to 20% after the water immersion process.

Peaks related to fluorine could be detected on the plasma-treated PMMA samples, as shown in Figure 4b, showing the XPS F1s high-resolution spectra of the plasma-treated surfaces shown in Figure 4a. There are two main F1s peaks. The first component at 687.5 eV is related to a covalent bond. The second component at 684.2 eV originates from the ionic-F bond, which is attributed to metal fluoride. While the first component at 687.5 eV increased after water immersion, the second component at 684.2 eV decreased significantly, as shown in Figure 4b. The Cr2p spectra with a range of 570–595 eV showed a similar reduction after the

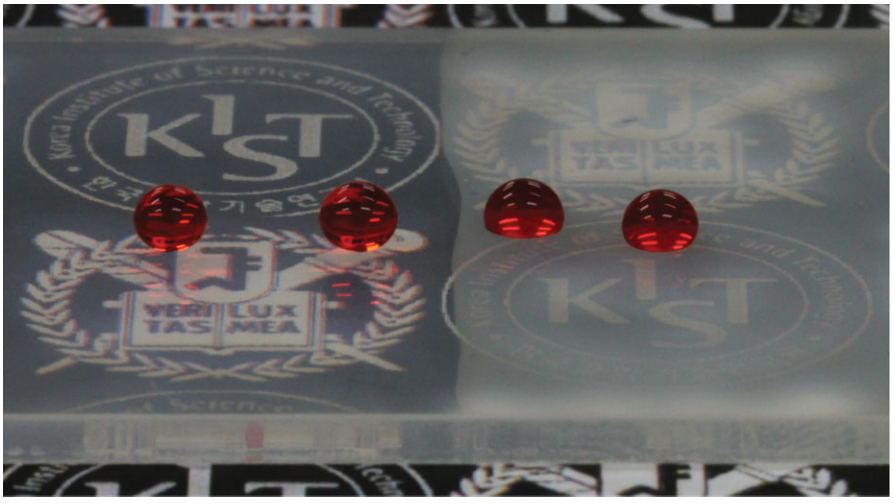

Figure 3. An optical image of one CF_4 plasma-treated and hydrophobic-coated sample on which the left half underwent the hydrolysis process and shows more transparency and hydrophobicity than the right half, which was completed without the hydrolysis process.

DOI: 10.1002/ppap.201200131

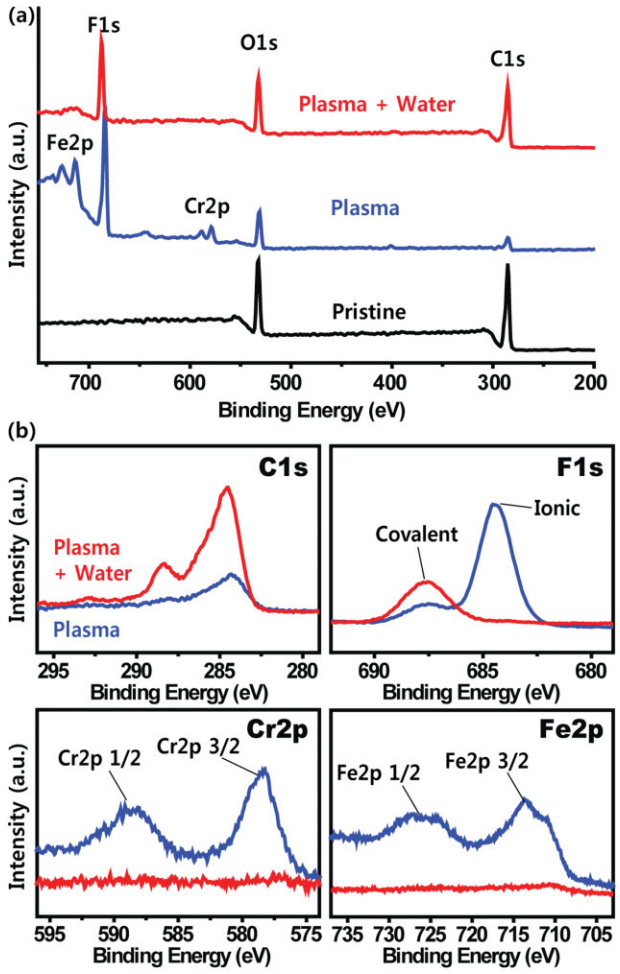

Figure 4. XPS analysis of PMMA surfaces for three different conditions: pristine, only a plasma treatment for 30 min and a plasma treatment for 30 min followed by water immersion. (a) XPS survey scan, and (b) high-resolution XPS spectra of C1s, F1s, Cr2p, and Fe2p.

water immersion step, as shown in Figure 4b. There are two components related to Cr2p 1/2 and Cr2p 3/2 located at 587.5 and 577.3 eV, respectively.[21] After the water immersion process, both peaks were significantly reduced. Likewise, the Fe2p spectra with a range of 705–735 eV showed a significant reduction of the Fe2p 1/2 and Fe2p 3/2 components after the water immersion step. These results indicated that the water immersion process could remove metal fluoride compounds through the hydrolysis reaction. These reactions were indirectly confirmed by the measurement of the pH value using a pH meter. The pH value of the water produced from the hydrolysis reaction with 15 samples that were treated for 30 min by CF_4 plasma was reduced from 6.9 to 3.9 in the case of DI water. The reduction of the pH value is indirect evidence of the formation of HF in DI water.

3.3. Water Wetting Behavior (CA and CAH)

The results of measurements of the static CA and CAH of sessile water drops on PMMA samples with various plasma durations with or without the hydrolysis process are shown in Figure 5. The flat surface of the pristine PMMA had a static CA of 71°, revealing its mild hydrophobic nature. As the hydrophobic SiO_x–C:H film was deposited to reduce the surface energy, the static CAs on the flat PMMA increased from 71° to 91°. The CF_4 plasma-treated PMMA given a hydrophobic coating without a hydrolysis process showed a range of CAs which increased from 112° to 141° owing to the increase in the roughness. Upon CF_4 plasma etching, nanostructures formed on the PMMA surface and the aspect ratio of the nanostructure increased with respect to the plasma treatment duration, as shown in Figure 1. For the plasma-treated PMMA surfaces followed by hydrophobic coating with hydrolysis, the CA increased from 119° to 159° and the CAH was significantly reduced from 90° to 3°, showing a lower CAH for a longer duration of the plasma treatment. This reduction of the CAH after the hydrolysis process originated from the lower value of the solid fraction

Table 1. Atomic concentration (at.-%) of CF_4 plasma treated PMMA.

CF_4 plasma duration [min]	Water immersion	Atomic concentration [at.-%]				
		C	O	F	Cr	Fe
Pristine	–	74.1	25.9	–	–	–
20	×	17.76	18.09	48.05	3.39	12.28
	○	60.17	20.07	17.94	0.61	0.72
25	×	17.46	17.8	48.88	3.41	11.72
	○	62.88	18.98	17.92	0	0
30	×	16.06	16.68	51.15	3.44	11.48
	○	59.67	19.7	19.98	0.02	0.62

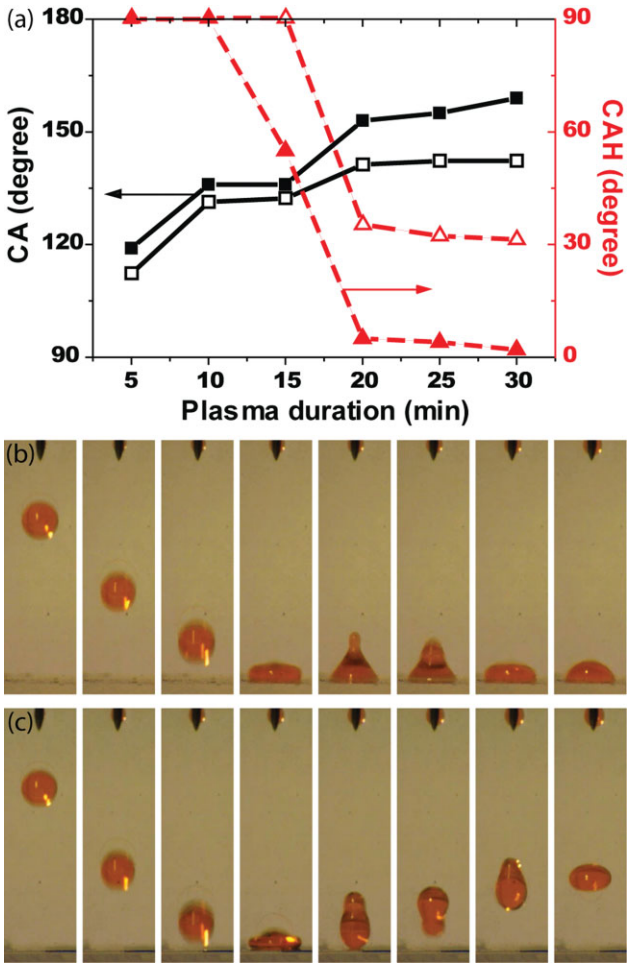

Figure 5. (a) CA and CAH of plasma-treated PMMA surfaces with different plasma durations. Plasma-treated PMMAs without (open marks) and with (solid marks) hydrolysis. High-speed camera images of falling water droplets with red dye on plasma-treated PMMAs (b) without and (c) with hydrolysis.

compared to that observed with the plasma-treated PMMA without hydrolysis. Representative high-speed camera images of water droplets falling on the hydrophobic PMMA surfaces without and with the hydrolysis reaction are presented in Figure 5b and c, respectively. Note that the droplet sits briefly and bounces on the surface after the hydrolysis process, showing superhydrophobicity. However, the falling water droplet becomes pinned to the surface without hydrolysis due to the higher solid fraction with the capping layer, indicating a higher CAH, as shown in Figure 5a.[22]

3.4. Water Condensation Behavior

When the condensed droplets coalesce, it is possible to deduce the mobility of a water droplet on the surface by observing the coalescence behavior. If the droplet has low mobility with a high CAH, a liquid film will form during the condensation process. Otherwise, when the droplet has high mobility with a low CAH, dropwise condensation behavior will prevail.[23,24] Here, we explored the water condensation behavior on hydrophobic PMMA and superhydrophobic PMMA using ESEM. Both samples were etched by CF_4 plasma for 30 min and coated with SiO_x–C:H for 5 s, but the latter sample underwent a hydrolysis reaction, while the former one did not. As shown in Figure 6a, a cluster-like condensation of water droplets occurs on the hydrophobic PMMA surface (without the hydrolysis process) under a super-saturation condition. The condensed water droplets adhere onto the surface and eventually coalesce with neighboring droplets. When the droplets coalesce, they maintain a contact line between the water and the solid surface owing to the low mobility of the water droplets, as denoted by the blue-dotted line in Figure 6a. This phenomenon derives from the high CAH and results in large-area contact between the water and the solid surface in a process known as film-wise condensation.[23] On the other hand, dropwise condensation occurred on the surface of the hydrophobic PMMA with the hydrolysis process, as shown in Figure 6b. Upon nucleation, the water droplets grew and coalesced with neighboring droplets. When coalescence occurred, the shape of the droplet remained circular, as denoted by the red-dotted circles in Figure 6b, where the droplets cover a small area and have high mobility. Therefore, it can be understood that the low solid fraction on the nanostructured surface also given the

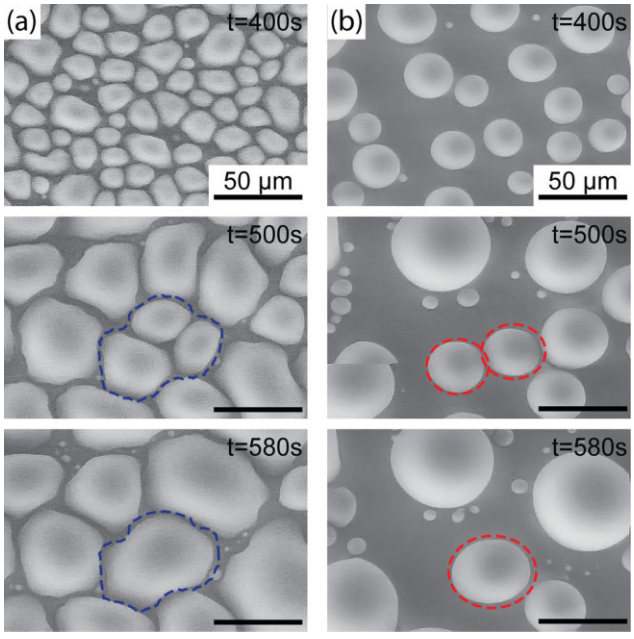

Figure 6. Micro-water droplets formed on CF_4 plasma-treated surfaces (a) without and (b) with hydrolysis at 5.6 Torr taken in ESEM.

DOI: 10.1002/ppap.201200131

hydrolysis process would enhance the hydrophobicity even during condensation.

To determine the internal liquid pressure of a droplet, we used the Young–Laplace equation, which relates the pressure difference (Δp) across the gas–liquid interface to the surface tension and the interface curvature, as expressed by $\Delta p = \gamma((1/R_1) + (1/R_2))$, where R_1 and R_2 are the principal radii of curvature. For a spherical water drop when $R_1 = R_2 = R$, we can reduce the formula to $\Delta p = 2\gamma/R$.[25] The smallest observed droplet had a radius of 5.3 μm at a pressure of 5.6 Torr and maintained a CA larger than 90°. From the measurement of the drop radius on the superhydrophobic PMMA with hydrolysis, the hydrophobicity could be maintained at least up to 27 kPa, which is much higher than the threshold pressure of 250 Pa for a millimetric water drop under compression,[26] and over which the transition from the Cassie–Baxter state to the Wenzel state may occur.[25]

3.5. Optical Transparency

Optical transparency, along with superhydrophobicity, is often a requirement for many applications, such as optical lenses, windows and solar cells. On the other hand, roughening is often required to improve the degree of hydrophobicity, but this reduces transparency.[11,27,28] The key question here is how to control the nanotexture to maintain transmittance for a specific wavelength range without sacrificing hydrophobicity.

Generally, the energy of transmitted light is equal to the difference in the incident energy and the reflected energy, ignoring absorption and scattering.[29] When the incidence light strikes in a normal direction from air to a solid surface, the reflectivity is explained with Fresnel equation:

$$R = \left(\frac{n-1}{n+2}\right)^2$$

here, n is the refractive index (RI) of the surface structure. In our case, we can assume that the surface structure is a composite consisting of air and solid components. Therefore, it is necessary to employ a proper model, such as an effective medium approximation. With this method, the RI of a surface structure which consists of a solid surrounded by air (RI = 1) is obtained as follows:[29]

$$\frac{(n^2-1)}{(n^2+2)} = f\frac{(n'^2-1)}{(n'^2+2)}$$

In this equation, n' is the RI of the solid and f is the corresponding volume fraction of the solid ($0 \le f \le 1$. From these equations, it is clear that the reflectivity is diminished when the volume fraction of the solid decreases.

Figure 7a and b show the transmittance in the range of 300–800 nm for pristine PMMA and eight treated samples coated with the hydrophobic coating. A comparison of the transmittance spectra of the pristine PMMA before and after the hydrophobic coating process indicates no significant decrease in the transparency of the PMMA. In Figure 7a, the samples were treated with CF_4 plasma for various durations, subsequently showing a hydrophobic film coated onto their surfaces. For short etch times, the surface remains transparent, while for longer etch times, the surface becomes milky. The transmittance of the samples decreased drastically with an increase in the plasma duration. The diameter of the capping layer on the nanostructures increased with an increase in the plasma duration, eventually exceeding the wavelength, as revealed in Figure 1 (left column). However, the transmittance of the PMMA surfaces with the hydrolysis reaction, shown in Figure 7b, was clearly improved because the capping layers on the nanostructures decomposed during the hydrolysis reaction. After 30 min of the plasma treatment, the transmittance of the samples gradually decreased to below 85% when comparing to air at a wavelength of 550 nm. This decrease is due to the aggregation of the PMMA pillar structures with a higher aspect ratio, as shown in Figure 1.

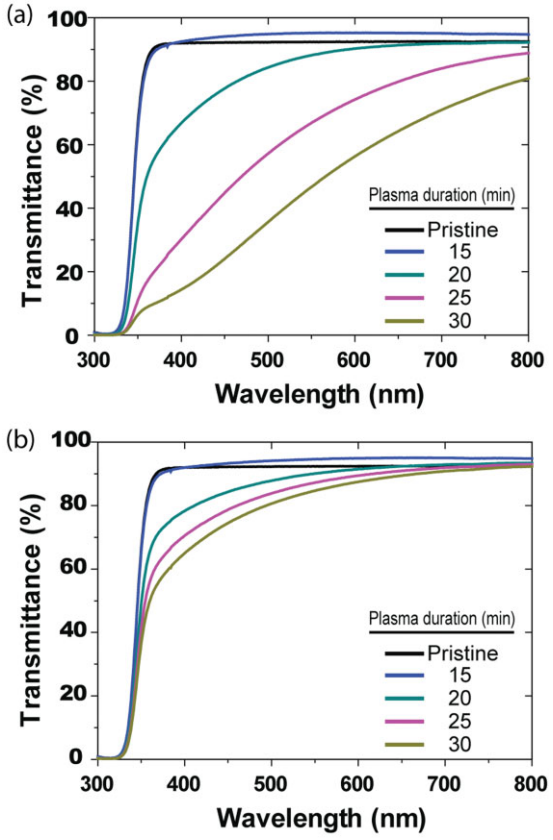

Figure 7. Measured transmittance in the 300–800 nm range for plasma-treated PMMA samples with different plasma durations: (a) without hydrolysis and (b) with hydrolysis.

4. Conclusion

A method to create a self-cleaning, transparent surface was presented. It forms nanostructures with a high aspect ratio on PMMA by utilizing a CF_4 plasma treatment/hydrolysis process followed by a hydrophobic surface coating. It was found that the CF_4 plasma treatment produced pillar structures on the PMMA surface but also formed a capping layer of metal fluoride, which could be removed through a hydrolysis reaction by a simple water immersion process. As a result, upright high-aspect-ratio pillars, the sizes of which are smaller than the optical wavelength in visible light, were achieved on the treated PMMA surface. With a hydrophobic coating following the hydrolysis reaction, superhydrophobicity of the surfaces was achieved, as shown by a water CA of 160° and non-sticky conditions (or CAH $<5°$). Optical transparency was also maintained, up to 95%, on the superhydrophobic surfaces. While maintaining their transparency, it was found that the surfaces formed with the hydrolysis reaction sustained strong superhydrophobic, or self-cleaning, behavior against wetting and dewing, as confirmed by water condensation experiments. Because the plasma-based surface modification and hydrolysis water treatment are both common and environmentally friendly processes, this method which improves the self-cleaning ability and maintains good transparency can expand the application of PMMA in various fields, such as smart windows, solar cell panels, and biomedical devices.[30]

Acknowledgements: This work was partially supported from the Global Excellent Technology Innovation R&D Program by the Ministry of Knowledge Economy (MKE), a project No. 10040003 funded by the MKE, and the Ministry of Education, Science and Technology (R11-2005-065, OKH). This work was also funded by an Eco-innovation program (Environmental Research Laboratory; 414-111-011 MWM) as well as by a KIST internal project.

Received: September 18, 2012; Revised: February 8, 2013; Accepted: February 11, 2013; DOI: 10.1002/ppap.201200131

Keywords: hydrolysis; hydrophobic coatings; plasma etching; poly(methly methacrylate) (PMMA); transparency

[1] S. Guruvenket, G. R. S. Iyer, L. Shestakova, P. Morgen, N. B. Larsen, G. Mohan Rao, *Appl. Surf. Sci.* **2008**, *254*, 5722.
[2] U. Schulz, P. Munzert, N. Kaiser, *J. Adhes. Sci. Technol.* **2010**, *24*, 1283.
[3] N. Vourdas, A. Tserepi, E. Gogolides, *Nanotechnology* **2007**, *18*, 125304.
[4] M. C. Almazan-Almazan, J. I. Paredes, M. Perez-Mendoza, M. Domingo-Garcia, F. J. Lopez-Garzon, A. Martinez-Alonso, J. M. Tascon, *J. Colloid Interface Sci.* **2005**, *287*, 57.
[5] K. Tsougeni, A. Tserepi, V. Constantoudis, E. Gogolides, P. S. Petrou, S. E. Kakabakos, *Langmuir* **2010**, *26*, 13883.
[6] J. L. Mauer, J. S. Logan, L. B. Zielinski, G. C. Schwartz, *J. Vac. Sci. Technol.* **1978**, *15*, 1734.
[7] M. D. Henry, S. Walavalkar, A. Homyk, A. Scherer, *Nanotechnology* **2009**, *20*, 255305.
[8] B. S. Kim, S. Shin, S. J. Shin, K. M. Kim, H. H. Cho, *Nanoscale Res. Lett.* **2011**, *6*, 333.
[9] R. Di Mundo, M. Ambrico, P. F. Ambrico, R. d'Agostino, F. Italiano, F. Palumbo, *Plasma Process. Polym.* **2011**, *8*, 239.
[10] R. Di Mundo, F. Palumbo, R. d'Agostino, *Langmuir* **2010**, *26*, 5196.
[11] A. Kaless, U. Schulz, P. Munzert, N. Kaiser, *Surf. Coat. Technol.* **2005**, *200*, 58.
[12] R. Di Mundo, M. Troia, F. Palumbo, M. Trotta, R. d'Agostino, *Plasma Process. Polym.* **2012**, *9*, 947.
[13] T. G. Cha, J. W. Yi, M. W. Moon, K. R. Lee, H. Y. Kim, *Langmuir* **2010**, *26*, 8319.
[14] T.-Y. Kim, B. Ingmar, K. Bewilogua, K. H. Oh, K.-R. Lee, *Chem. Phys. Lett.* **2007**, *436*, 199.
[15] Y. Rahmawan, M. W. Moon, K. S. Kim, K. R. Lee, K. Y. Suh, *Langmuir* **2010**, *26*, 484.
[16] I. D. Tevis, S. I. Stupp, *Nanoscale* **2011**, *3*, 2162.
[17] W. Dai, T.-J. Ko, K. H. Oh, K.-R. Lee, M.-W. Moon, *Plasma Process. Polym.* **2012**, *9*, 975.
[18] E. K. Her, H. S. Chung, M. W. Moon, K. H. Oh, *Nanotechnology* **2009**, *20*, 285301.
[19] Y.-H. Ting, C.-C. Liu, S.-M. Park, H. Jiang, P. F. Nealey, A. E. Wendt, *Polymers* **2010**, *2*, 649.
[20] P. Gröning, O. Küttel, M. Collaud-Coen, G. Dietler, L. Schlapbach, *Appl. Surf. Sci.* **1995**, *89*, 83.
[21] E. Kim, S. Hong, J. D. Gorman, S. Lim, S.-Y. Moon, D.-W. Kim, K. No, *Thin Solid Films* **1998**, *324*, 292.
[22] D. Bartolo, F. Bouamrirene, É. Verneuil, A. Buguin, P. Silberzan, S. Moulinet, *EPL (Europhys. Lett.)* **2006**, *74*, 299.
[23] B. J. Briscoe, D. R. Williams, K. P. Galvin, *Colloids Surf. A* **2005**, *264*, 101.
[24] T.-J. Ko, E. K. Her, B. Shin, H.-Y. Kim, K.-R. Lee, B. K. Hong, S. H. Kim, K. H. Oh, M.-W. Moon, *Carbon* **2012**, *50*, 5085.
[25] B. Shin, K.-R. Lee, M.-W. Moon, H.-Y. Kim, *Soft Matter* **2012**, *8*, 1817.
[26] A. Lafuma, D. Quéré, *Nat. Mater.* **2003**, *2*, 457.
[27] R. Di Mundo, V. De Benedictis, F. Palumbo, R. d'Agostino, *Appl. Surf. Sci.* **2009**, *255*, 5461.
[28] Y. Wang, N. Lu, H. Xu, G. Shi, M. Xu, X. Lin, H. Li, W. Wang, D. Qi, Y. Lu, L. Chi, *Nano Res.* **2010**, *3*, 520.
[29] S. Chattopadhyay, Y. F. Huang, Y. J. Jen, A. Ganguly, K. H. Chen, L. C. Chen, *Mater. Sci. Eng. R: Rep.* **2010**, *69*, 1.
[30] R. G. Karunakaran, C. H. Lu, Z. Zhang, S. Yang, *Langmuir* **2011**, *27*, 4594.